Article ID: 1007-4627(2016) 02-0146-06

New Generation of Experiments for the Investigation of Stellar (p,γ) Reaction Rates Using SAMURAI

V. Panin[1], K. Yoneda[1], M. Kurokawa[1], J. Blackmon[2], Z. Elekes[3], D. Kim[4], T. Motobayashi[1], H. Otsu[1], B. C. Rasco[2], A. Saastamoinen[5], L. Sobotka[6], L. Trache[7], T. Uesaka[1]

(*1. RIKEN Nishina Center, 2-1 Hirosawa, Wako, Saitama 351-0198, Japan;*
2. Louisiana State University, 211-A Nicholson Hal, Tower Dr., Baton Rouge, LA 708030-4001, USA;
3. MTA Atomki, Bem tér 18/c H-4026 Debrecen, Hungary;
4. Ewha Womans University, Seoul, South Korea;
5. Texas A&M University, USA;
6. Department of Chemistry, Washington University, Saint Louis, MO, 63130, USA;
7. IFIN-HH, str. Reactorului 30, Bucharest-Magurele RO-77125, Romania)

Abstract: The future experimental campaign with the SAMURAI setup at RIKEN will explore a wide range of neutron-deficient nuclei with a particular focus on the most critical (p,γ) reaction rates relevant to the astrophysical rp-process in type-I X-ray bursts (XRB). Intense radioactive-ion (RI) beams at an energy of a few hundred MeV/nucleon will be deployed to populate proton-unbound states in the nuclei of interest through the Coulomb excitation or nucleon-removal processes. The decay of these states into a proton and a heavy residue will be measured using complete kinematics and the information about time reversal proton-capture process will be obtained. This method will provide the vital experimental data on the resonances, which dominate the stellar (p,γ) reaction rates, as well as on the direct proton-capture process for some other cases. The experimental setup will utilize for the first time the High-Resolution 90°-mode of the SAMURAI spectrometer in combination with the existing detection systems, including custom-designed Si-strip detectors for simultaneous detection and tracking of heavy ions and protons emitted from the target. The details of the experimental method and the utilized apparatus are discussed in this paper.

Key words: type-I X-ray burst; rp-process; (p,γ) reaction rate; neutron-deficient RI beam
CLC number: O571.6 **Document code:** A **DOI:** 10.11804/NuclPhysRev.33.02.146

1 Subject and motivation

Explosive hydrogen burning at extreme temperature and density conditions is one of the most fascinating topics in modern nuclear astrophysics, which only in the last decades became accessible for detailed experimental studies due to availability of intense neutron-deficient radioactive-ion (RI) beams. Such exotic nuclear species in the proximity of the proton drip-line play an important role in the astrophysical rp-process - a dominating nucleosynthesis path in type-I X-ray bursts (XRB) which are often referred as the most frequent type of thermonuclear explosions in the Galaxy[1–3].

XRBs are recurrent events originating from close binary star systems due to thermonuclear runaway at the surface of a neutron star which accretes H/He-rich matter from an adjacent low-mass donor star[1]. When critical temperature ($T \approx 1 \sim 2$ GK) and density ($\rho \approx 10^6$ g/cm^3) are reached in the hot envelope of the neutron star, the explosive process is triggered by 3α-reaction followed by a sequence of (p,γ) and (α,p) reactions (αp-process) promoting the burning material into the $A = 40$ region[4]. After that, a rapid sequence of (p,γ) reactions and β-decays occurs (rp-process), thus processing the abundance flow further along the proton dripline with an extension all the way into $A \approx 100$ region[5–6] where the nucleosynthesis is

Received date: 30 Oct. 2015;
Foundation item: OTKA project (114454)
Biography: Valerii Panin (1985–), male, Alchevsk, Ukraine, Ph.D., working on experimental nuclear physics;
E-mail: valerii.panin@riken.jp.

believed to stop in the closed SnSbTe cycle due to disintegration of α-unbound isotopes $^{106-108}$Te. The entire process lasts typically $10 \sim 100$ s and results in an excessive yield (factor of about 10) of X-ray photons emanated from the neutron star's surface. This phenomenon is usually observed as a fast X-ray flash with a characteristic shape of the light curve. A wealth of information about properties of a neutron star such as mass, radius, spinning frequency *etc.*, can be extracted from the XRB light curves[3, 7], if the underlying nuclear process is correctly described in the framework of an accurate fluid dynamics model.

The main difficulty in studying XRB nucleosynthesis arises from its complexity - several hundreds isotopes and thousands nuclear interactions can be involved in a single XRB event. However, experimental information is very scare for most of them and theoretical calculations may yield uncertainties of a factor of $10 \sim 100$ for some reaction rates that, in turn, leads to significant discrepancies in the predicted XRB properties such as energy generation rates, light curves and resulting final chemical abundances[8–9]. The final chemical abundances can be essential, in particular, for the cooling of the neutron star surface as well as for the consecutive bursts which develop on the preceding nuclear ashes[10]. It was found in the recent state-of-the-art sensitivity studies[3, 8–9], based on large (over 600 isotopes) network calculations and on various hydrodynamic models with different XRB conditions (accreation rate, temperature and density profiles, *etc.*), that about less than 50 reactions may have any significant effect on the XRB properties such as overall energy output and final chemical yields. Such reactions can be identified in the vicinity of the so called waiting point (WP) nuclei (^{30}S, ^{60}Zn, ^{64}Ge, ^{68}Se, *etc.*) for which successive adding of another proton is inhibited by negative or very low proton-capture Q-values (a few hundreds keV). In such case (p,γ) reactions are hampered by either proton decay or reverse photodisintegration (γ),p establishing (p,γ)-(γ),p equilibrium. In both situations the process must "wait" until the relatively slow β^+ decay to process towards heavier nuclei via adjacent isotonic chains. This may lead to accumulation of the material in the region of the WP-nucleus (Z,N) and thus define the resulting composition of the burned ashes as well as nuclear energy generation rates and profiles of the XRB light curves. Investigation of the identified most critical (p,γ) reaction rates is of primary importance for the experimental studies in the next years. It will also become the main focus of the future experimental campaign with the large-acceptance spectrometer SAMURAI, taking advantage of the most intense RI-beams in the world available at RI-beam Factory in RIKEN[11].

2 Reactions in focus and the experimental method

Based on the previous theoretical sensitivity studies and XRB model predictions, the following set of reactions has been selected for future experiments at SAMURAI.

2.1 Breakout from WP-nuclei ^{64}Ge and ^{56}Ni

(a) ^{65}As(p,γ)^{66}Se

The reaction rate is found amongst the most influential for the final chemical yields of XRB[3, 9]. This is mainly due to its bridging effect on WP-nuclei ^{64}Ge, which, in most of the studied models, is a starting points towards production of heavier elements but is also a limiting factor of the rp-process due to its β-decay life-time of 92 s being comparable to the typical time scale of the entire XRB process. A possible breakout can occur at certain density and temperature conditions even through the proton unbound nucleus ^{65}As due to its finite lifetime. Hence, sequential two-proton capture on the WP-nucleus can be much faster than the associated β-decay[12]. In this case, decay constant of the ^{64}Ge via two-proton capture can be expressed as follows[3]:

$$\lambda_{^{64}\mathrm{Ge}\longrightarrow^{65}\mathrm{As}\longrightarrow^{66}\mathrm{Se}} = F(N_\mathrm{p},T,j_\mathrm{i},G_\mathrm{i})\times \exp\left(\frac{Q_{^{64}\mathrm{Ge}\longrightarrow^{65}\mathrm{As}}}{kT}\right)\times\lambda_{^{65}\mathrm{As}\rightarrow^{66}\mathrm{Se}}\ , \quad (1)$$

where $F(N_\mathrm{p},T,j_\mathrm{i},G_\mathrm{i})$ is a function depending on proton density N_p, temperature T, nuclear spins j_i and normalized partition functions G_i (for i=^{64}Ge, ^{65}As and proton); $Q_{^{64}\mathrm{Ge}\longrightarrow^{65}\mathrm{As}}$ is a Q value for proton capture on ^{64}Ge and $\lambda_{^{65}\mathrm{As}\rightarrow^{66}\mathrm{Se}}$ is a decay constant of ^{65}As with respect to subsequent proton capture. It can be seen that the breakout is not governed by the rate of ^{64}Ge(p,γ)^{65}As reaction, but by its Q-value, and by the rate of ^{65}As(p,γ)^{66}Se reaction.

(b) ^{57}Cu(p,γ)^{58}Zn

Similarly to the previous case, the reaction can lead to the breakout from doubly-magic WP-nucleus ^{56}Ni via sequential proton capture[13]. Early network calculations assumed that the rp-process stops at ^{56}Ni due to its low proton capture Q-value of 695 keV and comparatively long β-decay lifetime ($\tau = 2.3\times10^4$ s). However, later calculations[4, 14] employing larger networks show that the rp-process may process well beyond ^{56}Ni region. Influence of this reaction rate on the final chemical yelds, nuclear enegy generation rates and on the XBR light curves is also discussed in the recent state-of-the-art sensitivity studies[3, 9].

In the experiment, proton unbound states of ^{66}Se and ^{58}Zn will be populated by neutron removal reactions from ^{67}Se and ^{59}Zn beams, respectively, incident on the Be target at an energy 250 MeV/u. Proton decay spectroscopy of these states will be performed in-flight using the SAMURAI setup as explained in Sect. 3.

2.2 Resonant reaction rates around WP-nucleus ^{34}Ar

(a) ^{34}Ar(p,γ)^{35}K

Together with ^{30}S, the WP-nucleus ^{34}Ar was theoretically linked to the phenomenon of the multiple-peaked structure observed in some X-ray bursts[15]. Since the rates near the proton drip line can be significantly affected by isolated resonances[16], the identification of these states are important together with the determination of resonance energies ($E_{\rm R}$) and strengths ($\omega\gamma$), which are the only nuclear physics inputs into the resonant part of thermonuclear reaction rate. There is no experimental information on the resonance strengths, only shell model calculations are available to evaluate this reaction rate.

(b) ^{35}Ar(p,γ)^{36}K

When varied by a factor greater than 3, the reaction rate was found to significantly affect the calculated nuclear energy generation rate in the theoretical models[17]. The dramatic impact of ^{35}Ar(p,γ)^{36}K rate on XRB light curves had also been previously demonstrated by Thielemann[18]. Resonance strengths are not measured for this reaction yet.

(c) ^{35}K(p,γ)^{36}Ca

The reaction rate was identified by Amthor[19] as one of the 12 proton capture rates with an impact on predicted light curves. This rate was also found to affect predicted nuclear energy generation rates in the study of Ref. [17]. Presently, only the energy of one excited state is known in ^{36}Ca[20], and this state with tentative spin-parity assignment is the sole input considered in rate evaluations to date. so far.

The above three reactions will be studied via coulomb dissociation of ^{35}K, ^{36}K and ^{36}Ca beams inside lead target at 200 MeV/u beam energy. One- and two-proton decays in-flight of these nuclei will be measured to extract energies and strengths of the resonances relevant to the rp-process.

2.3 Direct proton capture reaction rates ^{27}P(p,γ)^{28}S and ^{31}Cl(p,γ)^{32}Ar

These reactions are predicted to be among 10 most important reaction[19] with the strong influence on the calculated XRB light curves. Both reactions rates are expected to be dominated by a direct proton capture, because no excited states at astrophysically relevant energies are known for ^{32}Ar and ^{28}S. Coulomb dissociation cross section of time-reversal processes ^{32}Ar$\rightarrow^{31}$Cl+p and ^{28}S$\rightarrow^{27}$P+p will be measured with lead target and 250 MeV/u beam energies to extract direct-capture components of the reaction rates. Complementary measurements of proton-removal reactions in the nuclear field (*e.g.* using ^{12}C target) will be additionally performed to extract Asymptotic Normalization Coefficients, which can be directly related to the direct-capture cross section. Combining the information from the both type of measurements would help to constrain the model uncertainties and to determine the reaction rates with higher accuracy.

2.4 Direct proton capture reaction rate ^{8}B(p,γ)^{9}C

The current knowledge of the rate of the ^{8}B(p,γ)^{9}C reaction in stellar conditions is contradictory at the best and there is no hope to determine it by other means than by indirect methods. This reaction gives a possible path to the hot pp chain pp-IV at high temperatures and away from it toward a rapid alpha process *rap* I at high temperatures and densities and therefore is important in understanding nucleosynthesis in super-massive hot stars in the early universe, including possible bypasses of the 3α-process[21]. Similar to the method described in subsection 2.3, breakup in nuclear and Coulomb fields at a beam energy of 300 MeV/u will be employed to estimate the direct-capture reaction rate.

3 Experimental appratus

3.1 SAMURAI setup

An overview of the intended experimental setup is shown in Fig. 1. Radioactive secondary beams will be produced by the fragmentation of primary stable beams (*e.g.* ^{78}Kr, ^{40}Ca or ^{16}O) at a few hundreds MeV/u energy in beryllium target and separated by BigRIPS fragment separator[11]. The particle identification of the beam will be then performed event-by-event using the $B\rho$-ΔE-TOF method. A secondary reaction target will be placed at the target position of the Superconducting Analyzer for MUlti-particles from RAdioIsotope Beams (SAMURAI)[22] and the incident beam will be focused on the target via superconducting quadrupole magnet STQ. Incident secondary beams will be measured in the tracking systems before the target with two scintillating detectors, SBT1 and SBT2, for time-of-flight measurements. The position of hit on the target and incoming angle of the secondary beams will be measured by two drift chambers (BDC1,2) placed upstream of the target. An ion-

ization chamber ICB will be used for charge identification of the incident ions. After traversing this pre-target section the beam is incident on the reaction target (beryllium, carbon or lead) inside the DALI2 γ-ray detector that will measure gamma-rays in coincidence with charged fragments. Directly after the target an array of Silicon Strip Detectors (SSDs) will be used to measure trajectories of outgoing protons and fragments. Due to the wide dynamic range of these detectors ($\sim 10^4$), simultaneous detection and tracking of a proton and a heavy ion is possible. The SSDs will provide vital information about relative angles between the fragment and the proton with a resolution of a few mrad, which determines to a large extent the invariant mass reconstruction and the corresponding relative energy resolution. Next, the SAMURAI spectrometer, rotated 90° with respect to the beam (High-Resolution mode) will separate the unreacted beam, breakup fragments and protons. The magnetic field will be set at around 2.8 T in the center of the spectrometer filled with helium gas at 1 atmosphere pressure. After the magnet, the protons are tracked by the two proton drift chambers, PDC1 and PDC2. The heavy fragments and the unreacted beam are measured in a separate drift chamber, FDC2. The time of flight and ΔE of the decay products are measured in two hodoscopes, labeled HODP and HODF, for the protons and the heavy fragments, respectively. Hence, identification and momentum measurement of every traversing particle will be performed and the invariant-mass analysis of the reaction products will be applied to reconstruct the decay energy of the initial system.

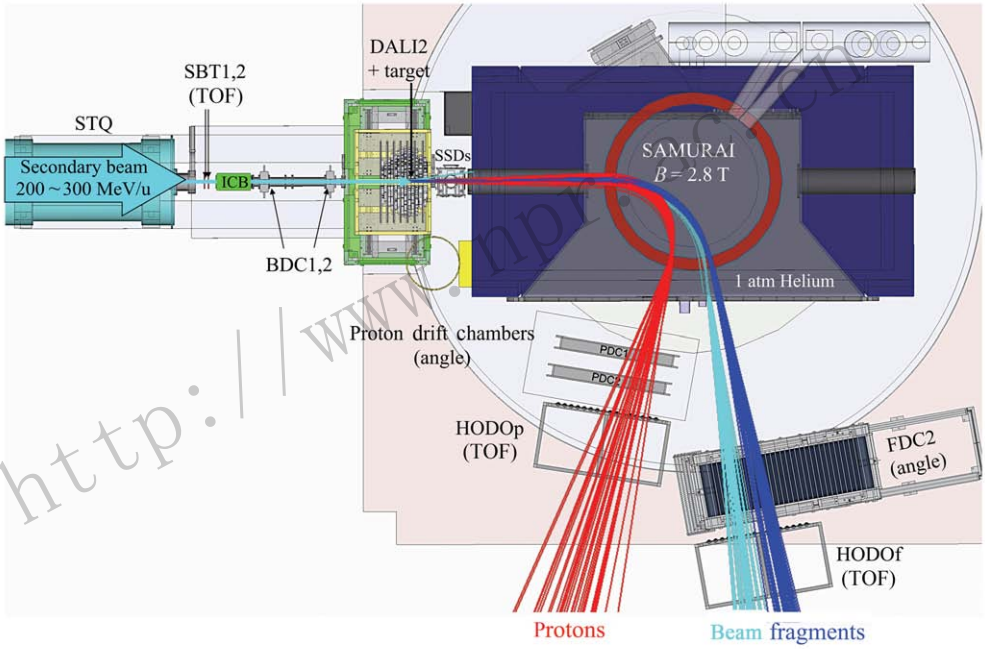

Fig. 1　(color online) High-Resolution (90°) mode of the SAMURAI setup will be used to measure heavy-ion-proton breakup reactions. Shown particle trajectories were simulated with Geant4 for the case of ^{28}S→^{27}P+p breakup. See text for more details.

3.2　Silicon strip detectors

An essential component of the setup will be an array of GLAST-type[23] single-sided Silicon Strip Detectors (SSDs) situated downstream of the target. Each detector is 325 μm thick and has dimensions of 87.6 cm×87.6 cm with 864 μm readout pitch size. Outgoing protons and heavy residues will be measured in the SSDs in order to reconstruct their relative angles with the precision of a few mrad. A key feature of the detectors is their wide dynamic range, which allows for simultaneous detection of protons and heavy ions, depositing in a single SSD a few hundred keV and up to 1 GeV energy, respectively. This is achieved via custom-designed ASIC dual-gain preamplifiers coupled to the high-density processing circuit HINP[24].

A performance test of the SSDs was conducted at the HIMAC facility in Japan, using irradiation of the detectors by proton beams at different energies (from 150 to 230 MeV/u) as well as by heavy-ion beams at a few hundred MeV/u in order to confirm the designed dynamic range. The results of the performance test are summarized in Fig. 2. Good linearity of the low-gain readout was observed together with the deposited-

energy (dE) resolution of ∼1.4%. The performance of the high-gain readout with respect to proton beams was also confirmed, yielding a proton-detection efficiency of > 97% and the cross-talk ratio of ∼1%. Thus, it was confirmed that the dynamic range of the SSDs spans from ∼ 100 keV up to ∼ 1 GeV, which would allow simultaneous detection of protons and $Z \approx 50$ heavy ions in SAMURAI experiments.

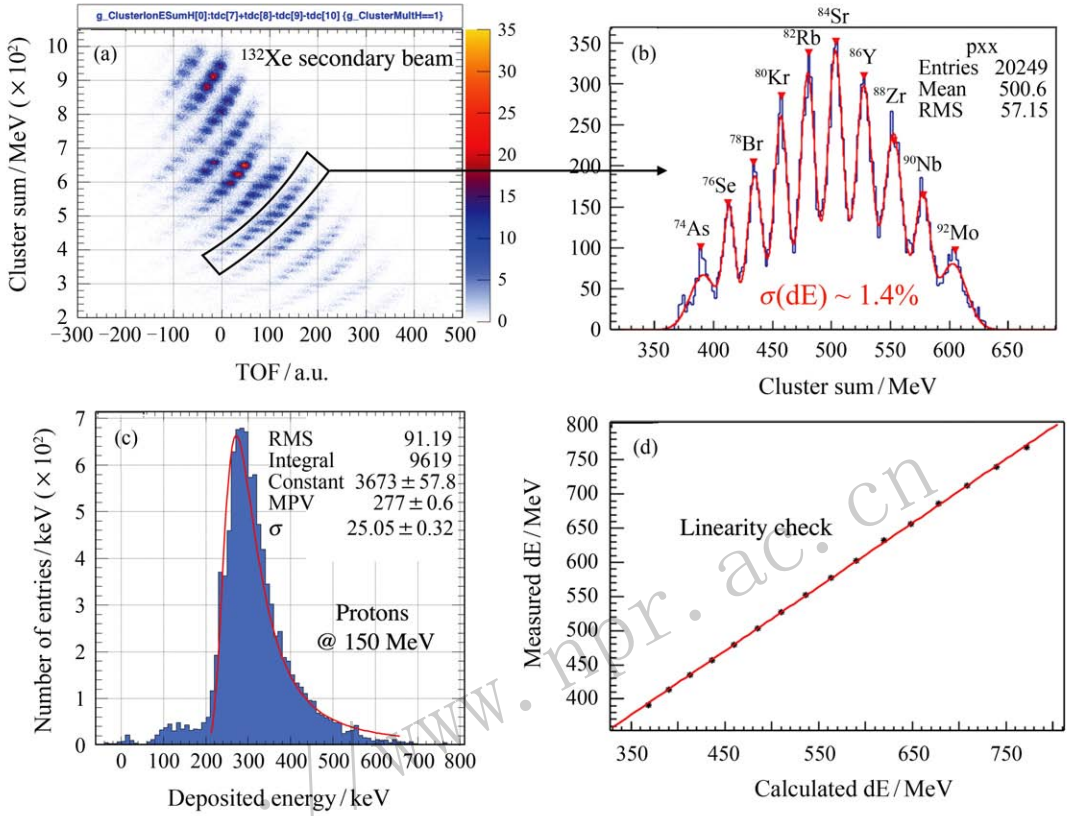

Fig. 2 (color online) Results of the performance test of the SSDs. Fig. (a) shows the particle identification of ^{132}Xe secondary beam, using the deposited energy (strip-cluster sum) measured by low-gain readout of the SSD as a function of the TOF. Fig. (b) shows the energy response in the SSD with the graphical cut indicated in Fig. (a), while Fig. (d) displays the linearity check for this energy range by plotting measured energies against the calculated ones. A signal form 150 MeV proton in high-gain readout of the same SSD is shown in Fig. (c) together with the Landau function fit.

3.3 Parameters of the experimental setup

Based on detailed Geant4 simulations of the particle transmission through the magnetic field of the SAMURAI spectrometer, and taking into account realistic detector responses, the following parameters of the setup can be estimated:

- Momentum resolutions: $P/\sigma_{\rm P} \approx 1300$ for heavy ions and $P/\sigma_{\rm P} \approx 500$ for protons;
- Angular resolutions: ∼3 mrad for protons and ∼2 mrad for heavy ions;
- Total detection efficincy: ∼100% for heavy ions and ∼20% for protons at relative energy $E_{\rm rel} = 1$ MeV;
- $E_{\rm rel}$ resolution ∼100 keV (σ) at $E_{\rm rel} = 1$ MeV.

4 Summary and outlook

The future experimental setup using SAMURAI spectrometer will serve as a powerful tool for systematic experimental studies of the most important (p,γ) reactions in the region of the astrophysical interest, using inverse and complete kinematics measurements of the heavy-ion-proton breakup reactions at relativistic energies. With the combination of the SAMURAI tracking detectors and the newly designed SSD trackers, possessing an extremely wide dynamic range, several neutron-deficient nuclei up to ^{100}Sn region can be potentially studied. The first experimental campaign will be ready to run in 2016, focusing on the proton decay of such exotic species as ^{66}Se, ^{58}Zn, ^{35}K, ^{36}K, ^{36}Ca, ^{28}S, ^{32}Ar and ^{9}C.

References:

[1] LEWIN W H G, van PARADIJS J, TAAM R E. Space Sci-

ence Rev, 1993, **62**: 223.
[2] WOOSLEY S E, TAAM R E. Nature, 1976, **263**: 101.
[3] PARIKH A, JOSE J, SALA G, *et al*. Prog Part Nucl Phys, 2013, **69**: 225.
[4] SCHATZ H, APRAHAMIAN A, GORRES J, *et al*. Phys Rep, 1998, **294**: 167.
[5] SCHATZ H, APRAHAMIAN A, BARNARD V, *et al*. Phys Rev Lett, 2001, **86**: 3471.
[6] KOIKE O, HASHIMOTO1 M, KUROMIZU R, *et al*. Astrophys J, 2004, **603**: 242.
[7] LEWIN W H G, van PARADIJS J, van den HEUVEL E P J, *et al*. Cambridge Univ Press, 1995: 175.
[8] PARIKH A, JOSÉ J, ILIADIS C, *et al*. Phys Rev C, 2009, **79**: 045802.
[9] PARIKH A, JOSÉ J, MORENO F, *et al*. New Astron Rev, 2008, **52**: 409.
[10] SCHATZ H. Int Symp Nucl Astrophys, Nuclei in the Cosmos IX, 2006.
[11] http://www.nishina.riken.jp/RIBF/.
[12] GÖRRES J, WIESCHER M, THIELEMANN F K. Phys Rev C, 1995, **51**: 392.
[13] FORSTNER O, HERNDL H, OBERHUMMER H, *et al*. Phys Rev C, 2001, **64**: 045801.
[14] van WORMER L, GORRES J, ILIADIS C, *et al*. Astrophys J, 1994, **432**: 326.
[15] FISKER J L, THIELEMANNET F K. Astrophys J, 2004, **608**: L61.
[16] SCHATZ H, BACHER A, BERG G P A, *et al*. Nucl Phys A, 1999, **654**: 924c.
[17] PARIKH A, JOSÉ J, MORENO F, *et al*. Astrophys J. 2008, **178**: 110.
[18] THIELEMANN F K, BRACHWITZ B, FREIBURGHAUS C, *et al*. Prog Part Nucl Phys, 2001, **46**: 5.
[19] AMTHOR A M. PhD thesis, Michigan State University, 2008.
[20] BÜRGER A, AZAIEZ F, ALGORA A, *et al*. Phys Rev C, 2012, **86**: 064609.
[21] WEISCHER M. Astrophys J, 1989, **343**: 352.
[22] KOBAYASHI T, CHIGA N, ISOBE T, *et al*. Nucl Instr Meth B, 2013, **317**: 294.
[23] BELLAZZINI R. Nucl Instr Meth A, 2003, **512**: 136.
[24] ENGEL G L. Nucl Instr Meth A, 2007, **573**: 418.